RESEARCH PAPER

Acta Neurobiol Exp 2020, 80: 1–18
DOI: 10.21307/ane-2020-001

Neuroprotective effect of poly(lactic-co-glycolic acid) nanoparticle-bound brain-derived neurotrophic factor in a permanent middle cerebral artery occlusion model of ischemia in rats

Siti Norsyafika Kamarudin[1], Igor Iezhitsa[1,2,3]*, Minaketan Tripathy[4], Renad Alyautdin[5] and Nafeeza Mohd Ismail[6]

*[1] Centre for Neuroscience Research, Faculty of Medicine, Universiti Teknologi MARA, Sungai Buloh Campus, Sungai Buloh, Selangor, Malaysia, [2] Institute for Pathology, Laboratory and Forensic Medicine (I-PPerForM), Universiti Teknologi MARA, Sungai Buloh Campus, Sungai Buloh, Selangor, Malaysia, [3] Research Centre for Innovative Medicines, Volgograd State Medical University, Volgograd, Russian Federation, [4] Centre for Molecular Pharmaceutics and Advanced Therapeutics, Adichunchanagiri College of Pharmacy, Adichunchanagiri University (ACU), B G Nagar, Karnattaka, India, [5] Scientific Centre for Expert Evaluation of Medicinal Products, Ministry of Health Russian Federation, Moscow, Russian Federation, [6] Faculty of Medicine, International Medical University, IMU Clinical School, Seremban, Malaysia, * Email: iezhitsa@yandex.ru*

Poly (lactide-co-glycolide) (PLGA) nanoparticles (NPs) are biodegradable carriers that participate in the transport of neuroprotective drugs across the blood brain barrier (BBB). Targeted brain-derived neurotrophic factor (BDNF) delivery across the BBB could provide neuroprotection in brain injury. We tested the neuroprotective effect of PLGA nanoparticle-bound BDNF in a permanent middle cerebral artery occlusion (pMCAO) model of ischemia in rats. Sprague-Dawley rats were subjected to pMCAO. Four hours after pMCAO, two groups were intravenously treated with BDNF and NP-BDNF, respectively. Functional outcome was assessed at 2 and 24 h after pMCAO, using the modified neurologic severity score (mNSS) and rotarod performance tests. Following functional assessments, rats were euthanized blood was taken to assess levels of the neurobiomarkers neuron-specific enolase and S100 calcium-binding protein β (S100β), and the brain was evaluated to measure the infarct volume. The NP-BDNF-treated group showed significant improvement in mNSS compared with pMCAO and BDNF-treated groups and showed improved rotarod performance. The infarct volume in rats treated with NP-BDNFs was also significantly smaller. These results were further corroborated by correlating differences in estimated NSE and S100β. NP-BDNFs exhibit a significant neuroprotective effect in the pMCAO model of ischemia in rats.

Key words: ischemia, neuroprotection, BDNF, brain infarct volume, neurological deficits, rotarod test, grid-walking test, neuron specific enolase, S100β protein

INTRODUCTION

Stroke remains a major health burden as the second leading cause of death worldwide, according to data published in 2012 by the World Health Organization. Annually, 15 million people worldwide suffer from stroke. Of these, 5 million die and another 5 million are left permanently disabled, placing the burden of care on the family and community (World Health Organization, 2002).

Stroke constitutes approximately 2 - 4% of total health care costs worldwide and accounts for more than 4% of direct health care costs in industrialized countries (Ga et al., 2008). Although the incidence and prevalence rates of stroke are decreasing in developed

Received 9 April 2019, accepted 23 October 2019

countries, the opposite trend is occurring in Asia Pacific, which has seen an increase in diagnosis of acute stroke (Aziz et al., 2015).

Clinically, stroke can be defined as an umbrella of conditions caused by the occlusion or haemorrhage of cerebral blood vessels supplying the brain (Lo et al., 2003). In both cases, stroke ultimately involves the death and dysfunction of neuronal cells and neurological deficits that reflect the location and size of the compromised brain area (Lo et al., 2003). To date, the only available treatment for acute ischemic stroke (AIS) patients with severe neurological deficits is to restore blood flow to the ischemic tissue with reperfusion therapies (Tsivgoulis et al., 2014). However, current therapies for AIS are inadequate, and the only approved medical therapy for AIS is tissue plasminogen activator (tPA), a thrombolytic agent that targets the thrombus within the blood vessel.

Neuroprotection remains one of the holy grails of AIS therapy. The ability to protect the ischemic brain from injury until reperfusion and also protect the brain from reperfusion injury could theoretically prevent disability in stroke survivors (Patel and McMullen, 2017). In the past, many neuroprotective agents showed efficacy in a variety of animal models of stroke, including 5-HT1A agonists, free radical scavengers, immunosuppressants, and excitotoxicity-blocking agents. However, despite efficacy in rodent models, most have failed in clinical trials (Mergenthaler and Meisel, 2012). Therefore, establishing new, effective neuroprotective strategies for AIS is an urgent concern.

One of the most promising neuroprotective agents is brain-derived neurotrophic factor (BDNF). BDNF is a neurotrophic protein that belongs to the neurotrophin protein family and is essential for central nervous system (CNS) development, neuronal survival, and neuronal plasticity (Han et al., 2013). It is the most prevalent growth factor in the CNS. Intracerebroventricular (ICV) infusion of BDNF was found to be neuroprotective in a permanent middle cerebral artery occlusion (pMCAO) model, provided that the ICV infusion of neurotrophin was initiated 24 hours prior to the ischemic insult (Schäbitz et al., 1997). Since it is necessary for BDNF to defuse from cerebrospinal fluid (CSF) into the layers of the brain following ICV infusion, BDNF is not neuroprotective without a significant lead-time before the ischemic insult. It is not practical to administer BDNF by ICV infusion for the treatment of AIS, much less 24 h before the ischemic insult. Neurotrophin needs to be delivered to the ischemic regions within the neuroprotective window period, which may be accomplished through the development of intravenously (IV) administered nanoparticle-based technologies that deliver BDNF after the ischemic insult.

The use of polymeric nanoparticles (NPs) as drug carrier to cross the blood brain barrier (BBB) and deliver BDNF to target cells will revolutionize the medical field. This technology could be applied to other neurological conditions, such as hypoxic ischemic insults, depression, Parkinson's disease, and Alzheimer's disease, in which BDNF has been proven beneficial using *in vivo* experiments (Nagahara and Tuszynski, 2011). Many studies have evaluated the effect of BDNF in hypoxic ischemia. Thus, it was beneficial to assess if BDNF could be neuroprotective against hypoxic ischemic injury in an ischemic stroke model (Chen et al., 2012; 2013a; 2013b; Han et al., 2013). Therefore, we designed BDNF-loaded poly (lactic-co-glycolic acid) (PLGA) NPs and studied the neuroprotective effects of PLGA NP-bound BDNF in a pMCAO model of ischemia in rats.

METHODS

Animals

Twenty-eight adult male Sprague-Dawley rats (250 g – 300 g) aged 8 to 10 weeks were obtained from the Laboratory Animal Care Unit of the Universiti Teknologi MARA (UiTM), Sg. Buloh Selangor. The animals were group-housed in plastic cages. The rats were placed in a room with a 12: 12 light-dark cycle and controlled temperature (23 ± 2°C). Food and water were accessible *ad libitum*. Prior to experimentation, rats were allowed to adapt to the environment for at least four days. Each rat was used once for all experiments. Animal handling and testing were carried out according to the procedures detailed in the Rodent Stroke Model Guidelines for Preclinical Stroke Trials (Liu et al., 2009). All experiments were approved by the Animal Ethics Committee of the Universiti Teknologi MARA (UiTM Care: 119/2015). All rats were randomly assigned into four groups (n=7 per group), which consisted of sham-operated (control, group 1), stroke (rats with permanent middle cerebral artery occlusion (pMCAO), group 2), BDNF-treated (rats with pMCAO treated with BDNF, group 3), and BDNF-loaded PLGA NPs (NP-BDNF) (rats with pMCAO treated with NP-BDNF, group 4) treated group.

Formulation and characterization of BDNF-loaded PLGA NPs

A total number of 10 µg of BDNF in 2 ml of Milli-Q water was poured into a solution of 500 mg of PLGA in 3 ml dichloromethane solution. The mixture was emulsified using a high shear rotor stator mixer. The obtained pre-emulsions were then added to 25 ml of 1%

aqueous solution of PVA and the mixture was passed through a high-pressure homogenizer (Next Generation Homogeniser, Nano DeBEE, USA) at 2,500 psi for 3 cycles. Then the organic solvent was removed using a magnetic stirrer and the emulsion was left for 24 h. Mannitol (5% w/v) was added to the resulting nanosuspension prior to being freeze-dried for 72 h. The PLGA NPs were coated with poloxamer 188 (PLX188) as a surfactant. For coating with PLX188 the lyophilized NPs were resuspended in a 0.01% w/v (optimal concentration) aqueous solution of PLX188.

The NP-BDNF was characterized for zeta potential, particle size, and morphological appearance.

NP size and zeta potential (ζ) were measured using a dynamic light scattering (DLS) technique (Malvern Zetasizer Nano ZS, UK). Approximately 0.3 ml of undiluted NP-BDNF solution was placed into a clear, disposable zeta cell, which was then inserted into the Zetasizer. The experiment was performed at room temperature (25°C) with a refractive index (η) of 1.33.

The morphology of the NP-BDNF was investigated with a transmission electron microscope (TEM) FEI TECNAI G2 20S TWIN and by environmental scanning electron microscopy (ESEM) FEI QUANTA 450 FEG (FEI Oregon, USA). For TEM, a sample of NPs was suspended in water (1mg/1ml). A drop of suspension NPs was placed onto parafilm and a copper grid was placed on top of the sample. The copper grid was left for 10 min followed by the addition of 2% (w/v) uranyl acetate, and then the samples were used for imaging. Pictures were taken at an excitation voltage of 200kV and a magnification of 6,000×. As for ESEM, the specimens were coated with a Pd-Au film by an Emitech Magnetron Sputter Coater before imaging in order to avoid electric charge build up. Pictures were captured at 16,000× magnification.

The entrapment efficiency (EE) of BDNF encapsulation in NP-BDNF was measured after removing excess BDNF and separating the particles using a modified minicolumn centrifugation method with Sephadex G-25 minicolumns. The experiment was repeated four times using the following procedure. In brief, Sephadex G-25 gel in the columns was allowed to swell with PBS for 15 min, followed by centrifugation for 5 min at 3,000 rpm to remove excess PBS. The dry column was loaded with empty PLGA NPs to saturate the column and minimize adsorption of actual samples. The loaded column was then centrifuged for 15 min at 3,000 rpm to expel the excess NPs. Next, NP-BDNFs were added to the column and centrifuged at 3,000 rpm for 15 min to separate untrapped BDNF from the NP-entrapped drug. The eluted sample containing entrapped BDNF-PLGA NPs was analysed for BDNF content. For this procedure, 20% Triton X was added to the sample to destroy PLGA NPs. Supernatant aliquots were taken and analysed for unbound BDNF using a human recombinant BDNF ELISA kit, with the absorbance set to 450 nm. The EE was calculated using the following formula:

$$Entrapment\ Efficiency\ (\%) = \frac{Entrapped\ drug}{Total\ drug} 100\%$$

Induction of ischemia by pMCAO

For this study, all rats were subjected to left side total pMCAO, using an intraluminal technique (Belayev et al., 1999). Rats were anesthetized with a mixture of xylazine (1.5 ml of 100 mg/ml) and ketamine (10 ml of 100 mg/ml) given intraperitoneally (0.1 ml/100g of body weight). After rats were deeply anesthetized, a ventral midline incision was created between the manubrium and the jaw on the left side of the neck. Then, blunt dissection was used to separate the superficial fascia and submandibular glands, and to expose the anterior triangle muscles of the neck, i.e., sternohyoid, sternomastoid, and digastric muscles. Once these muscles were identified, the blunt dissection was continued until the left common carotid artery (CCA) was exposed. The proximal area of the CCA and external carotid artery (ECA) were permanently ligated using 5-0 silk sutures. Meanwhile, the bifurcation of CCA was temporarily ligated with a loose knot (Koizumi et al., 1986). A microvascular clamp was applied to the internal carotid artery (ICA). A small arteriotomy was performed in between the permanent and loose ligation of the CCA. In order to create a thrombus or embolic lesion to induc e ischemia, a pre-prepared 4-0 nylon monofilament suture was inserted through the opening of the arteriotomy and was secured by tightening the loose ligation at the artery. Once the loose ligation was tightened, the microvascular clamp was removed, and the 4-0 nylon monofilament suture was rostrally advanced until it reached the ICA. The advancement of the suture was terminated once resistance was felt. This indicated that the blunted end of the suture reached the MCA and permanent occlusion was achieved. Finally, the midline incision of the neck was sewn with 3-0 silk using simple interrupted sutures. Postoperatively, the rat was placed in an individual nursing cage at 37°C to recover from the anesthesia. Once the rat regained consciousness from the surgery, it was then moved to a normal cage with *ad libitum* access to water and food.

Modified Neurological Severity Score (mNSS)

The mNSS test was used to assess impairment in all stroke model rats. The mNSS has a defined scoring sys-

tem, with 0 as the minimum score and 18 as the maximum score (Chen et al., 2001). After assessments, the total score was calculated and the severity of stroke was classified as follows: mild injury (1-6), moderate injury (7-12), severe injury (13-18), or no neurological impairment (0). Thus, the higher the score, the more severe the brain injury. The mNSS assesses motor, sensory, and reflex impairments in animal models after ischemic insults (Schaar et al., 2010). Stroke-induced motor deficits were assessed by the grid-walking test (Chao et al., 2010).

The grid-walking test

The grid-walking test was used for assessments of motor abnormalities in stroke rats. Each rat was placed on an elevated, metal, square-shaped grid unit. Each rat's performance was recorded for 5 min using a video camera (Handycam DCR-SX22E/B, Sony). A foot slip — when the paw completely missed a rung, when the limb fell between the rungs, or when the paw was correctly placed on the rung but slipped off during weight bearing — was considered to be an error of one limb climbing the grid. Foot slips and footsteps of the right and left forelimbs and hind limbs were counted. The motor impairment was expressed as a percentage of foot slips over footsteps for each rat. The findings were analysed by a person who was blinded to the experimental groups.

The rotarod performance test

The rotarod performance test was used to assess motor function and coordination after brain ischemia in rats. It consisted of a rotating rod onto which the subject was placed in order to evaluate motor impairment following brain insult. In this study the rats were trained on the rotarod prior to pMCAO. The training took three consecutive days, and during the training the rats had to perform three rotarod trials in a day with 30 min of rest in between the trials (Zhang and Pardridge, 2006). The speed of the rod was fixed at 16 revolutions per min (16 rpm). Any rats that were unable to stay on the rod for at least 200 s were excluded from the experiments. Rats were subjected to pMCAO on day 4, and on day 5 (24 h after pMCAO) the rats underwent the rotarod test, including three consecutive trials with 30 min of rest in between trials. The results were recorded as the average latency in seconds (s) (Zhang and Pardridge, 2006). During rotarod assessment, functional outcomes of the neurological impairment were recorded using a video camera (Handycam DCR – SX22F/B, SONY). A person who was blinded to the experimental groups evaluated the findings.

Infarct volume assessment using 2,3,5-triphenyltetrazolium chloride (TTC) staining

All rats were euthanized by terminal cardiac puncture. Prior to the procedure, the rats were anesthetized with a mixture of ketamine and xylazine. To reach the heart, a midline incision was made from the thoracic area down to the abdomen. Then, the abdominal muscles were separated until the heart was visualized. Blood was collected from the left ventricle using a 5 ml syringe with 18-gauge needle.

The rat was decapitated using a guillotine (NEMI Scientific Inc. USA). The brain was extracted and chilled in ice-cold saline (0.9% NaCl) for 2 min. Then, the brain was placed on an acrylic brain matrix (Ted Pella Inc, USA). Next, five coronal brain sections, 2 mm thick, were dissected at + 5, +3, + 1, –1, and –3 anterior–posterior from the bregma using sterilized disposable blades. Then, the slices were immersed in 0.05% 2,3,5-triphenyltetrazolium chloride (TTC) solution (Merck, USA) for 30 min at 37°C in a dark room (Joshi et al., 2004). The TTC-stained brain slices were placed on a glass slide. A millimeter scale ruler was placed beside the brain section to measure the stain area. The images of the slices were captured using a digital camera (Lumix DMC-S5, Panasonic) and analysed using ImageJ software (National Institutes of Health, USA). For each brain slice, the infarct area (mm^2) was estimated, and the total infarct volume (mm^3) was calculated by multiplying infarcted area by the 2 mm thickness.

The formula for calculating the infarct volume (mm^3) (Swanson et al., 1990) utilized an indirect method:

$$LI = RT - LN$$

where LI: infarct volume in the left hemisphere as measured by the indirect method, RT: total volume in the right hemisphere of the same brain, and LN: non-infracted cortex in the right hemisphere of the same brain.

Evaluation of S100 calcium-binding protein β (S100β) and neuron-specific enolase (NSE) levels by enzyme-linked immunosorbent assay (ELISA)

Two neuronal viability markers (NSE and S100β) were measured in serum using ELISA (USCN Life Science Inc.) to estimate the degree of cerebral tissue damage following pMCAO.

Serum was obtained from the 2.5 ml of blood collected by cardiac puncture. Each of the blood samples obtained was dispensed immediately in a BD Vacutainer® Rapid Serum Tube. The blood sample was allowed

to clot for one hour at room temperature prior to centrifugation at 1,000 x g for 20 min. The serum was collected and transferred to a clean tube. The serum was stored at -80°C until the time of analysis. The protein concentration of each serum sample was measured using a NanoDrop 1000 spectrophotometer (ND-1000 by Thermo Fisher Scientific, USA) and diluted 10-fold in 0.01 mol/L phosphate buffered saline (PBS) at pH 7 prior to the ELISA.

NSE and S100β standards were prepared by adding 1 ml of sample/standard dilution buffer into a standard tube to make 20 ng/ml of standard solution. After a 10-min incubation at room temperature, the standards were mixed thoroughly.

Prior to performing the assay, Horse-Radish Peroxidase (HRP) with Streptavidin-Biotin Complex (SABC) working solutions and 3,3′,5,5′-Tetramethylbenzidine (TMB) substrates were equilibrated for at least 30 min at 37°C. The samples and reagents were completely and evenly mixed. The standards, test samples, and control (zero) wells on the pre-coated plate were set and recorded, respectively. The plate was washed twice before addition of the standards, test samples, and controls. The standards and controls were aliquoted into the wells. Next, 0.1 ml of sample was added into the appropriate wells. The plate was sealed with a cover and incubated at 37°C for 90 min. After incubation, the plate contents were discarded, and the plate was clapped against absorbent filter papers or other absorbent materials. Next, 0.1 ml of biotinylated detection antibody working solution was added into the wells without touching the side of the wells. Then, the plate was sealed again and incubated at 37°C for 60 min. After the second incubation, the plate was washed three times with wash buffer. After the wash steps, 0.1 ml of SABC solution was added into each well, and the plate was again covered and incubated at 37°C for 30 min. Then, the cover was removed, and the plate was washed for five times for one to two min with wash buffer. After 90 µl of TMB substrate was added into each well, the plate was covered and incubated at 37°C in the dark for 15 to 30 min. Finally, 50 µl of Stop Solution was added into each well and mixed thoroughly. The OD was read at 450 nm in a microplate reader immediately after addition of the stop solution.

Statistical analysis

All results are presented as interquartile range. Data were analysed with the statistical package of social sciences software (SPSS) 21.0 for Windows (SPSS Inc., Chicago, IL). For comparison between multiple groups of parametric data, a one-way analysis of variances (ANOVA) was performed, followed by a *post-hoc* analysis using Bonferroni's test. For non-parametric data analyses, the Kruskal–Wallis test was performed to analyze significant differences between groups, followed by the Mann-Whitney test to compare between two groups separately. The mNSS were analysed using the Kruskal–Wallis followed by Mann Whitney test. One-way ANOVA, followed by Bonferroni's *post hoc* test, were used to analyze motor impairments in the rotarod and grid walking tests, infarct volumes, and levels of NSE and S100β. Differences at $p<0.05$ were considered statistically significant.

RESULTS

BDNF-loaded PLGA NPs

BDNF was incorporated into PLGA NPs, and subsequent coating with PLX188 was confirmed by particle size and zeta potential measurement.

Incorporation of BDNF increased the average size of the naked PLGA NPs from 27.8 ± 5.28 nm to 106.7 ± 3.42 nm, and the subsequent coating of NPs with PLX188 further increased the size to 186.6 ± 19.11 nm (Table I). The zeta potential decreased with the proce-

Table I. Physicochemical parameters of BDNF-loaded PLGA-nanoparticles (n=3).

Parameter	PLGA NPs	BDNF-loaded PLGA-nanoparticles (NP-BDNF)
Mean Particle size (nm)		
Before coating with PLX188	27.8±5.28	106.7±3.42
After coating with 0.01% (w/v) PLX188	160.7±8.41	186.6±19.11
Zeta potential (mV)		
Before coating with PLX188	-47.6	-20.8
After coating with PLX188	-34.3	-18.6
Entrapment Efficiency (%)		93%

dure described above. Drug encapsulation efficiency (EE) results demonstrated that BDNF had high loading capability into PLGA NPs. PLGA-NPs had a 93% EE. This indicates NP-BDNFs can act as an improved drug carrier. The enlargement of size and decreasing trend in zeta potential compliments each other. Furthermore, the trends in size are also supported by the imaging results (Fig. 1).

The morphological characteristics of the NP-BDNFs were observed using ESEM and TEM. The TEM images of NP-BDNFs (Fig. 1D) and empty NPs (Fig. 1B) show that the morphology of NPs were generally spherical, with particle sizes around 32.3-200 nm in diameter.

Effect of NP-BDNF on total brain infarct volumes (mm^3) of pMCAO-induced ischemic rats

The IV injection of NP-BDNFs decreased the infarct area of the NP-BDNF group, as seen in Fig. 2, compared

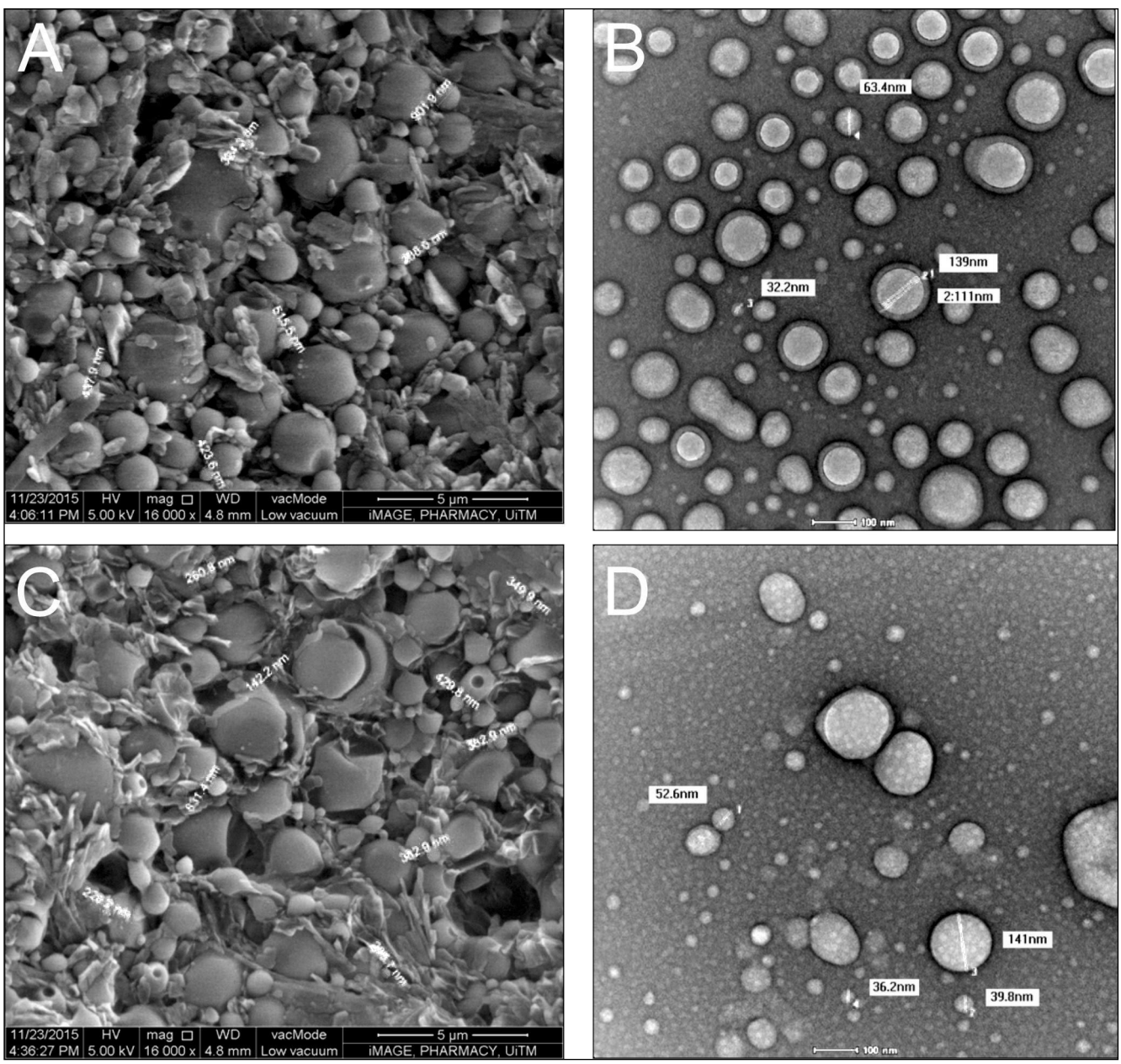

Fig. 1. The morphological characteristics of the NP-BDNFs observed using ESEM and TEM. (A) The ESEM image of PLGA NPs captured at 16,000× magnifications. (B) The TEM image of PLGA NPs. Pictures were taken at an excitation voltage of 200kV and a magnification of 6,000×; scale bar=100 nm. (C) The ESEM image of BDNF-encapsulated PLGA NPs after coating with PLX188 captured at 16,000× magnifications. (D) The TEM image of BDNF-encapsulated PLGA NPs coated with PLX188. Pictures were taken at an excitation voltage of 200kV and a magnification of 6,000×; scale bar=100 nm.

to stroke group and BDNF-treated group). Following TTC staining, the viable tissue was red and the infarcted area was white (Fig. 2). The sham-operated group showed no infarcted area.

The total brain infarct volumes (mm^3) of pMCAO-induced ischemic rats were estimated by summing up the infarct volume of each TTC-stained brain slice (Fig. 3), according to Swanson et al. (1990). The overall results showed significant differences among the groups (one-way ANOVA, *post hoc* Bonferroni's test, $F(3, 24)=123.02$, $p<0.01$). The total infarct volume was observed and measured in the stroke (204.95 mm^3), BDNF-treated (210.10 mm^3), and NP-BDNF-treated (107.58 mm^3) groups (Fig. 3). NP-BDNF-treated showed a significant 1.9-fold decrease in infarct volume ($p<0.001$) after the treatment with NP-BDNFs compared to the stroke group. When comparing infarct volumes between the BDNF-treated and NP-BDNF-treated groups, only the latter had a significantly lower infarct volume, by 2-fold ($p<0.001$), following the treatment. However, there was no significant difference between rats in BDNF-treated and stroke group.

Effect of BDNF-loaded PLGA NP on the functional neurological assessment of pMCAO-induced ischemic rats by mNSS

The mNSS test was carried out to assess neurological deficits following pMCAO and after post-treatment with either BDNF or NP-BDNF. The mNSS results were analysed using the Kruskal-Wallis test followed by Mann-Whitney-U test for pairwise comparisons across all the control and experimental groups ($F(3,42)=19.091$, $p<0.01$). The mNSS for the degree of ischemia in each group was estimated by the total score of all three mNSS components: the motor, somatosensory and reflex functions. The highest score was observed in the stroke group, which indicated that the rats suffered from a severe ischemic stroke. The test revealed that the mNSS score was significantly higher in the stroke rats by 14-fold ($p<0.001$) compared to the sham-operated rats (Fig. 4). Additionally, compared to sham group, the mNSS score was significantly higher in the pre-BDNF and pre-NP-BDNF-treated rats by 15- ($p<0.001$) and 14-fold ($p<0.001$), respectively, which indicates motor and somatosenso-

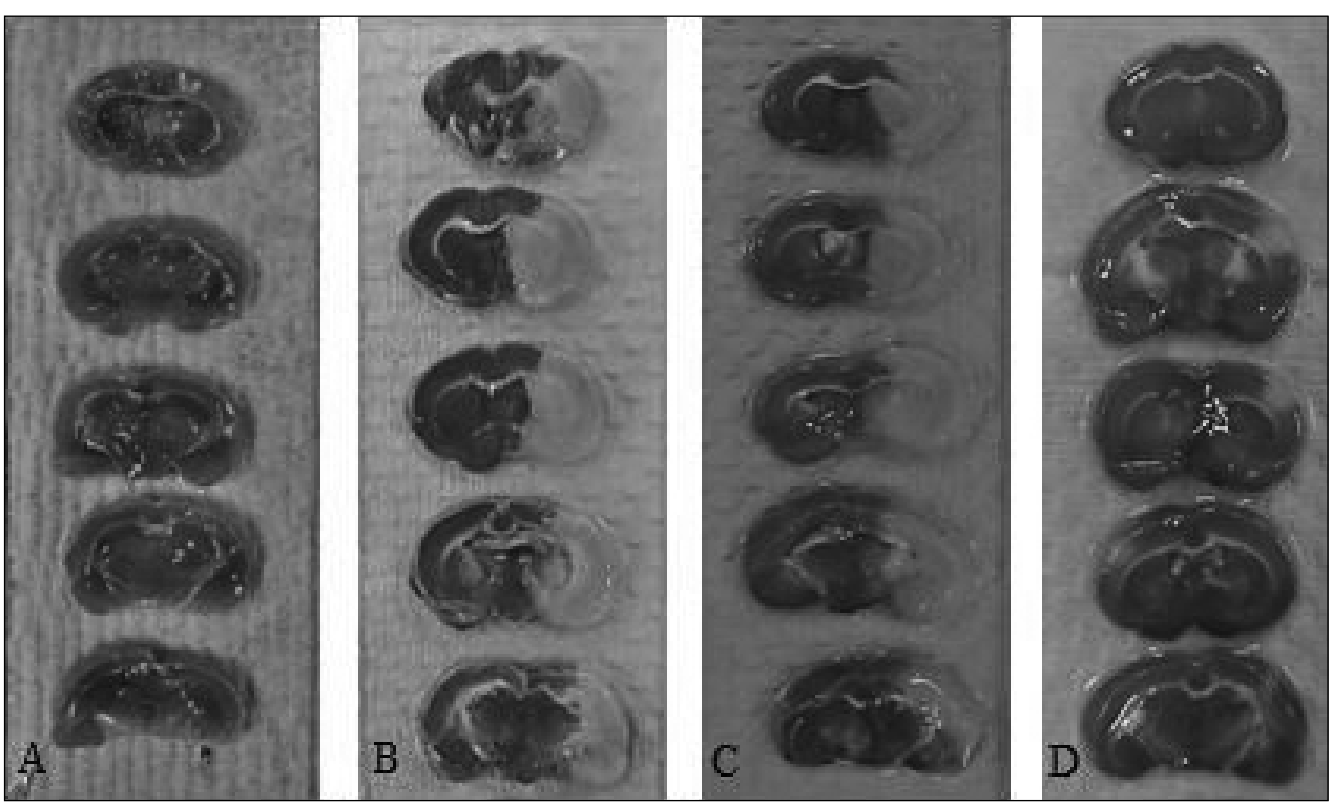

Fig. 2. Effect of BDNF-loaded PLGA NPs (NP-BDNFs) on the brain infarct area of pMCAO-induced ischemic rats. Immediate TTC staining shows deep red staining of normal brain tissue and white non-staining of the infarct tissue with distinct border. Representative TTC stains of coronal sections are shown for (A) Sham/control operated, (B) Stroke, (C) Stroke treated with BDNF, and (D) Stroke treated with NP-BDNF groups. The viable tissue is red, while the infarcted area induced by the stroke procedure is white. In the image, group D has less infarcted area than the stroke and BDNF-treated groups.

ry dysfunction (Fig. 4). These dysfunctions reflected ischemic injuries to the caudoputamen and frontoparietal cortex regions. Both areas received blood supply from the middle cerebral artery and are important in motor function, perception, cognition, and spatial tasks. The mNSS score remained significantly higher in the post-BDNF-treated group by 14-fold (p<0.001), and was improved in the post-NP-BDNF-treated group by a 7-fold decrease (p<0.001), when compared with sham-operated rats (Fig. 4).

Effect of BDNF-loaded PLGA NPs on the hemiparesis of the limbs following pMCAO-induced ischemic stroke

The induction of ischemic stroke in the left hemisphere of the rat brain by pMCAO resulted in the hemiparesis of the right limbs (contralateral), while the left limbs (ipsilateral) were not affected. Latency to fall in the rotarod test was significantly lower in stroke, pre-BDNF, and pre-NP-BDNF-treated groups compared to the sham-operated group by 4.7- (p<0.001), 4.9- (p<0.001), and 6.1-fold (p<0.001), respectively (Fig. 5). IV injection of NP-BDNF four h after pMCAO significantly prolonged the latency to fall from the rotating rod by 2.4- (p<0.001) and 3.2- (p<0.001) fold as compared to stroke and pre-NP-BDNF-treated groups, respectively. The latency to maintain balance on the rotarod was 2.8-fold (p<0.001) times higher in the post-NP-BDNF group than in the post-BDNF group. There were no significant differences in rotarod performance between pre- and post-BDNF-treated groups ($F(5, 36)=407.92$, p<0.01).

The grid-walking test was performed to evaluate the effect of NP-BDNF on the hemiparesis of the limbs in pMCAO-induced ischemic rats. The percentage of foot slips was recorded for left (ipsilateral) and right (contralateral) limbs in sham, stroke, stroke post-treated with BDNF, and stroke post-treated with NP-BDNF 24 h after pMCAO-induced ischemic stroke. The results for each group were represented as the mean percentage of total foot slips over total footsteps of the forelimb and hind limb. Concurrent with the rotarod test data, the NP-BDNF group showed better performance in the grid-walking test, as the mean percentage of contralateral foot slips was significantly lower compared to the stroke and BDNF post-treated group.

The stroke group, pre-BDNF-treated, and pre-NP-BDNF-treated groups showed a higher number

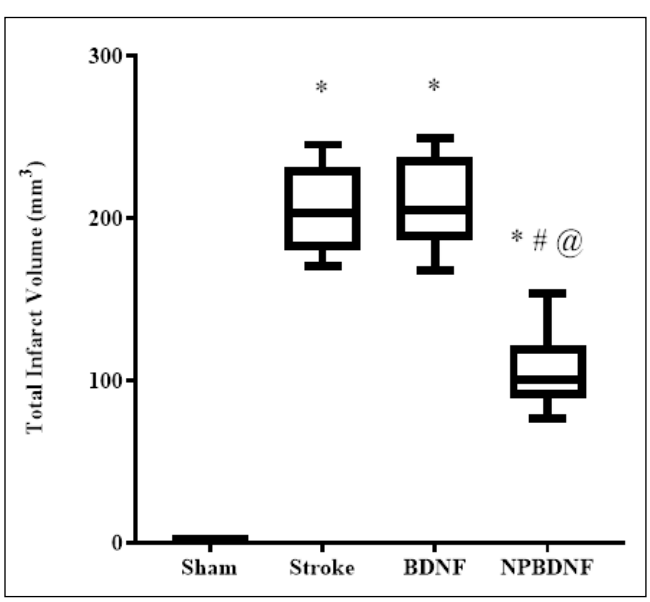

Fig. 3. Effect of BDNF-loaded PLGA NPs (NP-BDNF) on total infarct volumes (mm^3) of pMCAO-induced ischemic rats. Notes: Data is expressed as interquartile range. The box signifies the upper and lower quartiles, and a short black line within the box represents the median. Statistical significances were analysed using one-way ANOVA, followed by the Bonferroni *post hoc* test: n=7; *p<0.001 *vs.* sham, #p<0.001 *vs.* stroke, @p<0.001 *vs.* BDNF.

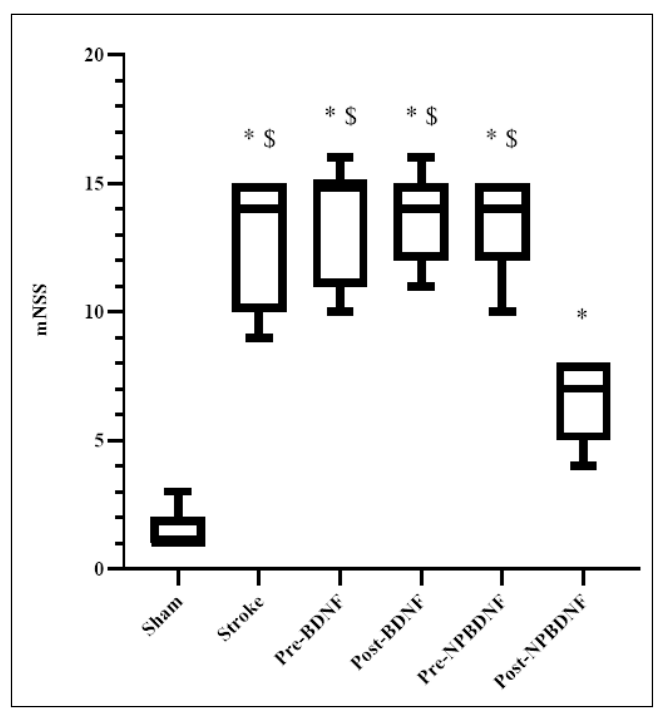

Fig. 4. Effect of BDNF-loaded PLGA NPs (NP-BDNF) on modified neurological severity scores (mNSS). Notes: Data is expressed as interquartile range. The box signifies the upper and lower quartiles, and the median is represented by a short black line within the box. Statistical analysis was performed using the Kruskal-Wallis test followed by the Mann-Whitney U test: n=7, *p<0.001 *vs.* sham, $$p$<0.001 *vs.* post-NP-BDNF. Pre-BDNF–stroke rats before receiving BDNF treatment; Post-BDNF–stroke rats after receiving BDNF treatment; Pre-NP-BDNF–stroke rats before receiving NP-BDNF treatment; Post-BDNF–stroke rats after receiving NP-BDNF treatment.

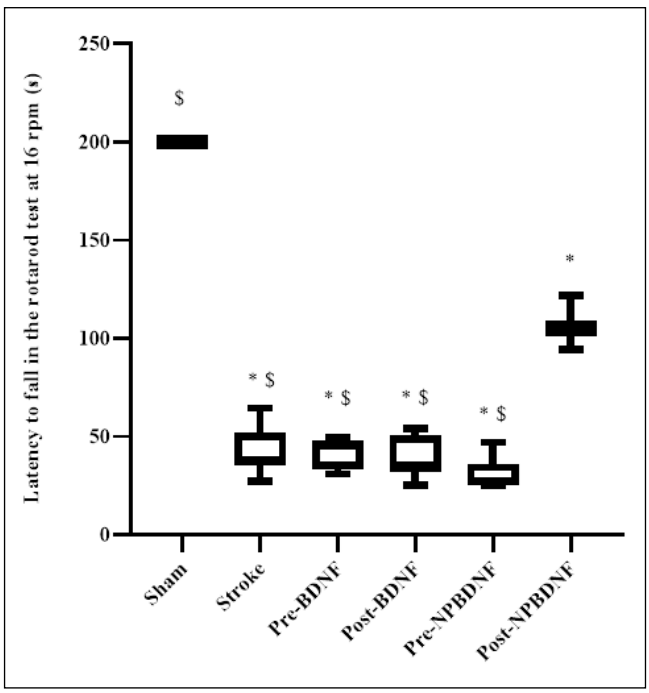

Fig. 5. Effect of BDNF-loaded PLGA NPs (NP-BDNF) on the functional motor assessment by the rotarod test. Notes: Data is expressed as interquartile range. The box signifies the upper and lower quartiles, and the median is represented by a short black line within the box. Statistics were analysed using the one-way ANOVA, followed by the Bonferroni *post hoc* test. n=7; **p*<0.001 *vs.* sham, $^{\$}p$<0.001 *vs.* post-NP-BDNF.

of errors in the right (contralateral) limbs compared to sham-operated rats by 15.1- (p<0.001), 15.3- (p<0.001), and 14.8-fold (p<0.001), respectively (Fig. 6) (Ipsilateral = F(5,36)=3.189, p<0.05; Contralateral = F(5,36)=29.716, p<0.01). Stroke rats treated with NP-BDNF showed marked error reduction in the number of right (contralateral) limb slips compared to stroke group, pre-BDNF-treated, post-BDNF-treated, and pre-NP-BDNF-treated groups by an average of 2-fold (p<0.001). No significant difference was observed in the percentage of left (ipsilateral) foot slips between all the study groups (p>0.05) (Fig. 6).

Effect of NP-BDNF on the concentration of serum neurobiochemical markers NSE and S100β

Effect of NP-BDNF on NSE levels

NSE is a CNS tissue injury biomarker for brain damage commonly used in animal and human studies, particularly following ischemic brain injury. The stroke, BDNF, and NP-BDNF groups exhibited higher mean NSE levels by 17- (p<0.001), 17- (p<0.001), and 10-fold (p<0.001), respectively, compared with the sham group (Fig. 7).

There was a significant reduction in NSE levels in the NP-BDNF group by 1.68-fold (p<0.001) compared to the stroke group and by 1.7-fold (p<0.001) compared to the BDNF group. However, NSE levels remained significantly higher in the NP-BDNF group by 10-fold (p<0.001) when compared with the sham group. There was no significant difference in NSE levels between BDNF-treated and stroke rats (p>0.05) (F (3,24)=6193.08, p<0.01).

Effect of NP-BDNF on S100β levels

S100β is a calcium-binding protein primarily expressed by neuronal tissue. The protein is released

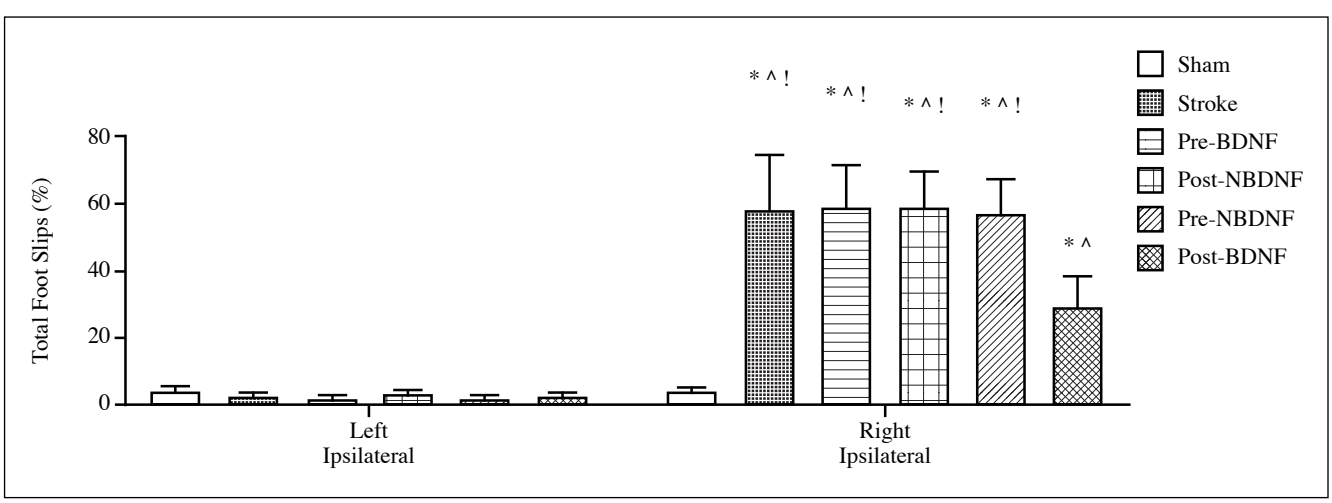

Fig. 6. Effect of BDNF-loaded PLGA NPs (NP-BDNF) on the percentage of contralateral and ipsilateral foot slips 24 h after pMCAO-induced ischemic stroke. Notes: Statistical analysis was performed using the two-way multivariate ANOVA, followed by the Bonferroni post-hoc test: n=7; **p*<0.001 *vs.* contralateral sham, $^{\wedge}p$<0.001 *vs.* respective ipsilateral, $^{!}p$<0.001 *vs.* contralateral post-NPBDNF; Pre-BDNF–stroke rats before receiving BDNF treatment; Post-BDNF–stroke rats after receiving BDNF treatment; Pre-NP-BDNF–stroke rats before receiving NP-BDNF treatment; Post-BDNF–stroke rats after receiving NP-BDNF treatment.

from cells following neuronal injury and can be detected in serum, urine, or CSF with a simple bioassay. It has thus been widely investigated as a potential biomarker for brain injury. S100β protein levels are significantly elevated in cases of traumatic brain injury, neonatal asphyxia, and injury secondary to cardiac arrest, as well as other neurodegenerative diseases.

The stroke, BDNF and NP-BDNF groups exhibited higher mean S100β levels by 98.1- (p<0.001), 98.6- (p<0.001) and 58.7-fold (p<0.001), respectively, compared to the sham group (Fig. 11). Following treatment, there was a significant reduction in S100β levels in the NP-BDNF group by 1.7-fold (p<0.001) when compared with stroke and BDNF-treated groups (Fig. 8). However, S100β levels were significantly lower in the sham-operated group by 55-fold (p<0.001) when compared with the NP-BDNF-treated group. There was no significant difference in S100β levels between the BDNF-treated and stroke groups (p>0.05) ($F(3,24)=914.702$, p<0.01).

DISCUSSION

This study has demonstrated the effectiveness of nanoparticulated BDNF as a neuroprotective agent following left pMCAO. We found that the reduction in infarct volume demonstrated the neuroprotective effects of BDNF after the treatment with NP-BDNF following ischemic injury, as BDNF blocked apoptotic cell death in the ischemic penumbra region. The ischemic penumbra consists of neurons that undergo active apoptotic death as a result of reduced blood flow to the neuronal cells. A previous study showed that BDNF exerts its neuroprotective effect by preventing caspase-3-mediated apoptosis in ischemic penumbra tissue (Kume et al., 1997; Barone and Feuerstein, 1999; Han et al., 2000).

For the first objective, the principal finding of this study was a significant reduction in infarct volume in the pMCAO stroke group treated with NP-BDNF, more so than in the other groups. This finding is in agreement with a previous study (Yamashita et al., 1997), Schäbitz et al., 1997). Meanwhile, the expression of BDNF was significantly increased in the peri-infarct cortices of MCAO-induced mice treated with direct AT2-receptor (AT2R) stimulation with the non-peptide AT2R-agonist compound 21; this was correlated with a reduced infarct volume and significantly decreased number of apoptotic neurons in the peri-infarct cortex of the mice (Schwengel et al., 2016). BDNF is a well-known neurotrophic agent with pleiotropic effects. It exerts its effects on brain function, including neuroprotection, vascular remodelling, neurogenesis, neuronal survival, and neuroplasticity, following injury to brain cells, particularly after ischemic insults (Chao, 2003; Ohira and Hayashi, 2009; Lu et al., 2013). Additionally, BDNF regulates neuronal survival, cell migration, and synaptic function (Thoenen, 1995; Murer et al., 2001; Baydyuk and Xu, 2014; Lu et al., 2014; Meng et al., 2019).

Another observation from this study was that both the stroke and BDNF-treated stroke groups showed extensive cerebral infarct volumes. these results are consistent with recent studies on pMCAO rat models, (Park

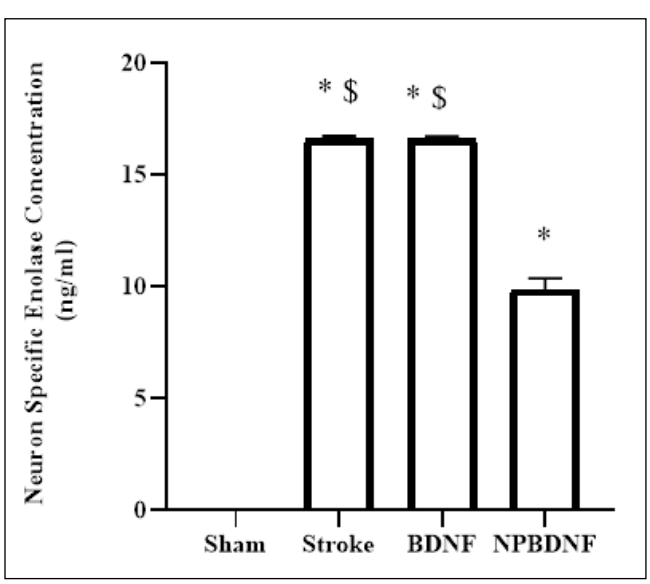

Fig. 7. Effect of BDNF-loaded PLGA NPs (NP-BDNF) on NSE serum levels in pMCAO-induced ischemic rats. Notes: Data are presented as mean ± SD. Statistics were analysed using the one-way ANOVA, followed by the Bonferroni *post hoc* test: n=7, *p<0.001 *vs.* sham, $^{\$}p$<0.001 *vs.* NP-BDNF.

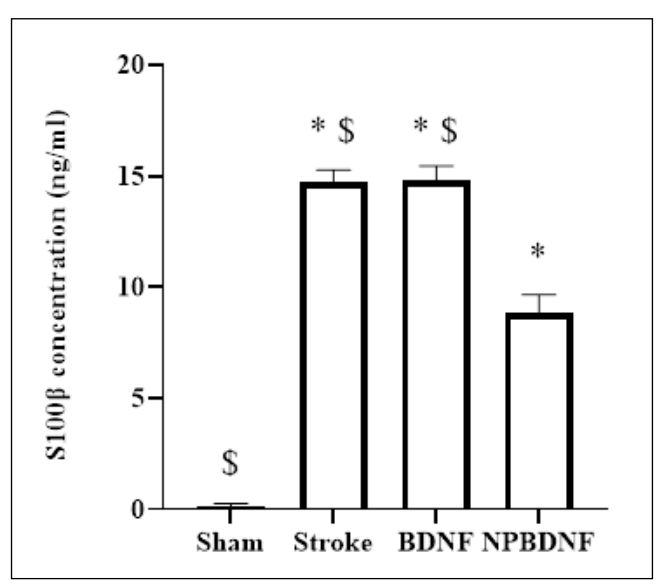

Fig. 8. Effect of BDNF-loaded PLGA NPs (NP-BDNF) on S100β concentration in serum. Notes: Data are presented as Mean ± SD. Statistics were analysed using the one-way ANOVA, followed by the Bonferroni *post hoc* test: n=7, *p<0.001 *vs.* sham, $^{\$}p$<0.001 *vs.* NP-BDNF.

et al., 2014) and 200 mm^3 (Kim et al., 2014). On the other hand, a slightly higher infarct volume (370 mm3) was observed when the ischemic stroke rats were induced with a 90-min transient MCAO (Wang et al., 2010). Typically, induction of MCAO leads to cell death predominantly in the striatum and extends into the parietal, temporal and frontal cortex areas. In addition, damage was also observed in the thalamus, hypothalamus, and substantia nigra (Garcia et al., 1995; Kanemitsu et al., 2002; Williams et al., 2004). In the same way, the brain damage of ischemic stroke rats in the present study covered a wide area of the striatum and cerebral cortex, starting from the rostral to the midline frontal cortex. Subsequently, widespread damage involving these brain areas was expected to manifest as disturbances to motor function, coordination, and somatosensory deficits as previously shown in behavioral studies.

Treatment with NP-BDNF significantly reduced areas of brain death, which were mainly located in the dorsolateral cortex that covers the striatum. Prior studies have described a consistent pattern of MCAO-induced cell death, which initially begins with striatal infarction and progresses towards the dorsolateral cortex that covers the striatum (Liu et al., 2009; Popp et al., 2009; Ejaz et al., 2013). One group reported the progression of the ischemic core and penumbra region following MCAO-induced stroke in a rat model that started at the spatiotemporal region (Carmichael, 2005). This present study hypothesizes that treatment with NP-BDNF provides neuroprotection that could salvage neuronal cells in the ischemic penumbra area, which lies mainly in the cortical region surrounding the ischemic core of the striatum.

The infarct volume is calculated based on the differences between red and white areas of the brain cortex after TTC staining. Although the TTC technique is common and convenient, a potential drawback has been described. Several studies have reported the occurrence of overlapping areas between viable and infarcted regions within the TTC-stained brain slices, which could result in inaccurate measurement of the total infarct volume (Garcia et al., 1996; 1997; Baron et al., 2014). Despite the limitations of the TCC-derived infarct volume, as a major marker of MCAO outcome in stroked rats its measurements of functional recovery reflect outcome better than infarct volume (Albers et al., 2001).

In the present investigation, IV administration of BDNF alone had no neuroprotective effect in regional brain ischemia. These results are in agreement with a study by Zhang and Pardridge in which saline-treated pMCAO animals showed no significant difference in infarct volume (2001). However, BDNF alone does have a neuroprotective effect following direct ICV administration (Yamashita et al., 1997), when the BBB is bypassed, or with IV administration in stroke models that have a disrupted BBB.

Lee et al. (2014) emphasized the importance of the duration of the arterial occlusion to stroke outcomes. They demonstrated that a 60-min transient occlusion produced moderate stroke severity, while a longer period, such as occlusion for 90 min, caused severe neurological deficits in rats (Lee et al., 2014). It is reasonable, then, to hypothesize that the neurological deficits seen in the 90-min transient MCAO were due to severe brain insults triggered by a longer occlusion as well as injury from the subsequent reperfusion. The cerebral damage in the 60-min transient MCAO model was equal to that of the permanent MCAO model and was less than the damage observed in the 90-min occlusion Moreover, previous studies demonstrated that pMCAO induces moderate neurological impairment, with a mean total mNSS score between 4 and 7 points using the 14-point scale (Chen et al., 2005; Oron et al., 2006; Boltze et al., 2012; Sun et al., 2015) and 10 points using the 18-point scale (Zhang et al., 2004; Li et al., 2005). Similarly, other studies demonstrated that a 60-min transient MCAO (Lee et al., 2012; Park et al., 2012; Lee et al., 2014) resulted in moderate stroke symptoms, with the mean total mNSS score between 8 and 11 points using the 18-point scale. The area of MCAO-induced cerebral infarction is often confined between the caudoputamen, temporal and occipital lobes, frontoparietal cortex, and a number of subcortical structures, such as the hypothalamus, in rats (Garcia et al., 1995; Kanemitsu et al., 2002). Hence, it is evident that pMCAO of the left-brain hemisphere induced moderate focal neurological impairments that mainly caused motor and somatosensory deficits, as reflected by the mNSS, without affecting other functions, such as reflexes and myoclonic movement.

NP-BDNF-treated ischemic rats demonstrated a mild form of stroke, as indicated by improved neurological functions and mNSS scores, compared to untreated stroked rats. On the other hand, BDNF-treated ischemic rats demonstrated a moderate form of stroke, similar to untreated ischemic rats. To date, many studies have explored the role of BDNF as a neuroprotective agent, particularly during ischemic insults. As in previous studies, we noted a reduction in stroke volume and an improvement in functional outcomes following delayed IV administration of BDNF in regional brain ischemia (Zhang et al., 2006). Improvement of neurological deficits in NP-BDNF-treated stroked rats was due to the ability of the NPs to carry BDNF across the BBB and exert its neuroprotective effects. This result occurred because the NP formulation that contained BDNF enabled receptor-mediated transport across an intact BBB *in vivo* (Zhang et al., 2006). Another study by Zensi et al. (2009) demonstrated that localization of NPs with co-

valently bound apolipoprotein E (Apo E) were detected in brain capillary endothelial cells and neurons after IV administration of human serum albumin NPs with covalently bound Apo E in mice. These findings indicate that NPs with covalently bound Apo E are taken into the cerebral endothelium by an endocytic mechanism, followed by transcytosis into the brain parenchyma. These similar results highlight the significance of the surface properties of NPs in successful and efficient brain drug delivery.

In this study PLGA NPs were coated with the PLX188 surfactant. Surface modification with PLX188 enabled the successful NP delivery of BDNF across the BBB. The PLX188 coating enhanced the penetration, as confirmed by other studies (Gelperina et al., 2010; Wohlfart et al., 2011; Kulkarni and Feng, 2011). Another essential point is that coating polymeric NPs with PLX188 decreases the clearance of NPs by the reticuloendothelial system thereby increasing the circulation time of the compound in the plasma (Moghimi and Hunter, 2000; Mozafari et al., 2009). This enhances NP delivery across the BBB, because the NPs are able to bind to the low-density lipoprotein receptor (LDLR) located on the surface of the BBB.

A number of behavioral assays were performed in rats prior to the pMCAO and after treatment either with BDNF alone or NP-BDNF, to confirm the neurological deficits associated with cerebral ischemia. Muscle weakness or motor impairment is a common complaint after stroke in humans. In this study, the results demonstrated a correlation between vestibulomotor recoveries, as measured by the rotarod and grid-walking tests, and neurocognitive function, as measured by mNSS scores, and showed reduced cerebral infarct volumes in animals treated with IV administration of NP-BDNF.

The severity of motor deficits correlated with the extent of cerebral infarction. A reduction in cerebral infarction areas resulted in improved functional motor recovery. A prior study showed that IV BDNF treatment after pMCAO reduced cerebral infarct size and counterregulated apoptotic proteins, particularly Bax and Bcl-2, after temporary focal cerebral ischemia (Schabitz et al., 2000). Subsequently, many researchers correlated the pathology results with behavior outcomes in MCAO models following neuroprotection with BDNF. Zhang et al. (2018a) concluded that neuroprotective neurotrophins, such as BDNF, improve functional outcomes following treatment with DPSCs combined with BDNF in rats with focal cerebral ischemia. On the other hand, Taliyan and Ramagiri (2016) found that lithium treatment upregulated BDNF expression after acute ischemic insults, and that this increase correlated with improved functional motor assessment in MCAO rats. Another study showed that BDNF may modulate local inflammation at cellular, cytokine, and nuclear factor levels in the brain after MCAO, and that this may reduce cellular injury caused ischemic insults and reduce neurologic deficits after stroke (Jiang et al., 2010). In the present study, in the pMCAO-induced ischemic stroke rats the rotarod latency significantly increased following treatment with NP-BDNF.

The third assessment, the grid walking or foot fault test, was a functional motor assessment to determine the degree of the hemiparesis (Hernandez and Schallert, 1988; Chao et al., 2012). In the present study, pMCAO rats exhibited the highest incidence of contralateral foot slips, compared to the other groups. This data is consistent with previous studies showing that ischemic animals generally demonstrate significantly more contralateral foot slips than normal healthy animals (Schaar et al., 2010). In this study, the observation of contralateral foot slips was likely due to pMCAO that caused primary motor and somatosensory impairment, as correlated by the mNSS scores and rotarod assessment. This finding was consistent with a number of studies, which demonstrated that the induction of pMCAO resulted in a significant increase in contralateral foot slips (Shukla et al., 2006; Chen et al., 2005; Rogers et al., 1997a). The duration of arterial occlusion also had an impact on the severity in neurological impairments. A study by Rogers et al. (1997a), reported the number of contralateral foot slips in rats with transient MCAO increased with the MCAO duration of the ischemic stroke that was induced in the left hemisphere of the rat brain; therefore, it affected right limb functions and the left limbs remained unaffected. In the present study, the ipsilateral limbs of stroked rats in each group demonstrated significantly lower incidences of foot slips compared to contralateral foot slips, indicating that the pMCAO procedure successfully induced specific focal strokes in the left-brain and caused hemiparesis of only the right limbs. The ischemic stroke rats in all groups, except for the sham-operated group, showed no significant difference in latency and frequency of movement during the grid-walking test prior to treatment. These results were in concordance with the mNSS results that showed that pMCAO induced altered latency in ischemic stroke rats with moderate to severe ischemia.

On the other hand, ischemic rats treated with NP-BDNF showed significant improvement in contralateral limb function; these results suggest that NP-BDNF was effective in rendering sensorimotor cortex protection against ischemia. Other than assessing coordination, the grid-walking test also assesses grip strength, which was not evaluated during the mNSS

motor tests. Overall, we postulated that treatment with NP-BDNF induced neuroprotection and restricted the spread of the infarction area from reaching the motor and somatosensory cortices of the rats.

NSE, or enolase-2, is a γγ isoenzyme of enolase that converts 2-phospho-glycerate to phosphoenolpyruvate, and is a glycolytic enzyme predominantly located in the cytoplasm of neurons and neuroendocrine cells. NSE represents a high percentage (1.5%) of total soluble brain proteins and is stable in biological fluids. It is also present in other non-neuronal sites, most notably erythrocytes. In normal subjects, however, it is only found in minor concentrations (Casmiro et al., 2005; Gelderblom et al., 2013). For that reason, increased serum NSE levels are a reliable neurobiomarker of the severity of neuronal damage and BBB impairment following insults. Many studies using animal stroke models have confirmed this significant increase in NSE (Horn et al., 1995; Yi et al., 2008; Gelderblom et al., 2013; Guo et al., 2014). According to Gelderblom et al. NSE (2013) is an exclusive biomarker of neuronal injuries because NSE was found in supernatants of lysed neurons and was absent in supernatants of lysed glial cells or in plasma of normal mice. Moreover, NSE levels were highly correlated with levels of lactate dehydrogenase, an enzymatic marker of cell death (Gelderblom et al., 2013). Furthermore, a study by Horn et al. (1995) further strengthened the argument that serum NSE could correlate with ischemic neuronal injury. They discovered that transient, bilateral occlusion for 5 minutes resulted in a significant increase in serum NSE concentration in the Mongolian gerbil ischemic stroke model. In addition, leakage of the disrupted BBB was evident in hypoxic ischemic rats that also had fewer NSE-positive cells in the cerebral cortex but increased serum NSE level (Yi et al., 2008).

Importantly, NSE is a neurobiomarker that can also identify neuronal injury in human subjects who have suffered brain insults, including cerebral infarction (Cunningham et al., 1991; Çakmak et al., 2014), subarachnoid hemorrhage (Mabe et al., 1991; Tawk et al., 2015), and head injury (Skogseid et al., 1992; Chabok et al., 2012; Olivecrona et al., 2015). The increased levels of blood NSE could be primarily attributed to loss of CNS NSE due to nerve damage (Çeltik et al., 2004; Gelderblom et al., 2013; Guo et al., 2014; Bharosay et al., 2018).

Tawk and colleagues (2015) found that an increased NSE level correlates with poor clinical presentations and worse outcomes following subarachnoid hemorrhage. One study demonstrated increasing NSE levels over several days in a small sample of ischemic stroke patients (Persson et al., 1987), and another study showed that the magnitude of serum NSE in hemorrhagic stroke was higher in patients with poor neurological status (Mabe et al., 1991). Moreover, the maximum levels of serum NSE detected were correlated with the severity of head injury (Skogseid et al., 1992) and cerebral infarct volume (Cunningham et al., 1991).

The disturbance in endothelial tight junctions of the BBB around the peri-infarct zone during traumatic brain injury, such as ischemic stroke, causes an increase in paracellular permeability (Haley and Lawrence, 2017). Due to this event, vascular-derived substances were allowed to enter the brain and brain-specific proteins could leak into the circulatory system (Sandoval and Witt, 2008). Moreover, the compromised BBB also played a role in the formation of edema that, consequently, worsened the neurological outcome (Stokum et al., 2016). In addition, another study further hypothesized that the ischemia associated with BBB dysfunction did not necessarily depend on the structural alteration of endothelial tight junctions (Krueger et al., 2013) but could also be assisted by transcellular pathways involving caveolae or vacuoles in the endothelium that lead to transcytosis of plasma proteins across the BBB (Zhang et al., 2015; Nahirney et al., 2016). Additionally, a number of studies reported significant correlations between the NSE levels in the circulatory system, brain infarction volumes (Li et al., 2015), and neurological deficits (Zaheer et al., 2013; Bharosay et al., 2018). Due to these data, an evaluation of BBB integrity is a crucial factor in determining the severity and progression of ischemic stroke injury.

In the present study, circulating NSE after cerebral artery occlusion was significantly increased in plasma following pMCAO-induced cerebral infarction, but not following sham surgery. The increased plasma NSE, under these conditions, corresponded to infarct volume and neurological impairment assessments, which included mNSS, rotarod, and grid-walking tests. The NSE levels were determined 24 h post-pMCAO induction. Following NP-BDNF treatment, NSE levels were significantly lower than in untreated pMCAO rats and BDNF-treated pMCAO rats. Reduced NSE levels correlated with the degree of neurological impairments, as assessed by neurobehavioral activity. IV administration with NPs containing neuroprotective agents, such as BDNF, resulted in lower NSE levels, reduced stroke volumes, and improved functional outcomes.

Similarly, S100β is another neurobiomarker that predicts prognosis after acute ischemia and indicates effectiveness of neuroprotective treatments (Tanaka et al., 2007; Mori et al., 2010). S100β is a glial-derived, calcium-binding, 21 kDa protein comprised of two subunits, A and B, that is involved in multiple intra-

cellular processes and functions as a neurotrophic factor. S100β is also involved in the regulation of intracellular and extracellular calcium metabolism. When the two subunits combine, they result in S100AB and S100BB subtypes. S100AB is predominantly found in astrocytes, S100BB is located in both Schwann cells and astrocytes, and S100AA is found in striated muscle, heart, and kidney (Tanaka et al., 2007). Application of S100β in nanomolar concentrations protected neurons against apoptosis, enhanced astrocytes, stimulated neurite outgrowth, and enhanced survival of neurons during development *in vitro* (Sorci et al., 2013). In contrast, micromolar levels of S100β stimulated nitric oxide synthase expression and nitric oxide secretion from cultured astrocytes (Hu et al., 1997; Matsui et al., 2002) and induced proinflammatory cytokines (Koppal et al., 2001) and neuronal apoptosis (Fulle et al., 2000; Steiner et al., 2011; Zhang et al., 2018b). S100β levels in serum or CSF significantly correlated with the brain infarct volume, neurological deficits, and functional outcome in patients with ischemic stroke and animal models of stroke (Missler et al., 1997; Elting et al., 2000; Tanaka et al., 2007; Nash et al., 2008). In this study, there was a significant increase in S100β levels in pMCAO rats and BDNF-treated pMCAO rats. S100β levels were reduced in NP-BDNF-treated rats, when compared with sham-operated rats. These results showed there was a significant effect of ischemic stroke on the level of S100β in the serum of untreated and BDNF-treated pMCAO rats. A previous study found that S100β levels significantly increased 24 h after a 60-min transient ischemic stroke in rats, and that S100β levels peaked at 48 h after the stroke. In this study, the level of S100β was measured 24 h after pMCAO. The elevation of the serum S100β correlated with the brain water content 72 hours after pMCAO, suggesting that S100β could be a neurobiomarker for the formation of brain edema and disruption of the BBB (Tanaka et al., 2007). Furthermore, the level of S100β at 48 h after MCAO could indicate the severity of the neurological impairments measured at 168 h after stroke (Tanaka et al., 2007). In the current study, the ischemic stroke group showed a significant elevation in serum S100β levels, which correlated with the degree of neurological impairment found in pMCAO and BDNF-treated pMCAO rats. Previous studies have described an association between the level of S100β and pathophysiological mechanisms relating to the formation of vascular injuries, BBB disruption, and edema (Tanaka et al., 2007). Numerous studies have also proven that samples drawn at later time points establish stronger correlations between serum biomarker concentrations and clinical or radiographic measures (Jauch et al., 2017).

CONCLUSION

This study successfully demonstrated the neuroprotective effect of NP-BDNF in pMCAO-induced ischemic stroke in rats for the first time. The optimal formulation, with ideal particle size and less negative surface charge, allowed NPs to penetrate the BBB efficiently. We found that the total infarct volume and levels of neurobiomarkers (NSE and S100β) were significantly reduced in rats with pMCAO when NPs were given at a BDNF concentration of 50 ng/ml during the window period (4 - 6 h) of neuroprotection. Thus, the behavioral and functional assessment of rats with ischemic stroke showed significant improvement after treatment with NP-BDNF.

ACKNOWLEDGEMENT

We acknowledge the administrative and facility support provided by the Centre for Neuroscience Research (NeuRon), the Institute of Medical Molecular Biotechnology (IMMB), the Laboratory Animal Care Unit (Faculty of Medicine) and the Laboratory of Fundamental Pharmaceutics (Faculty of Pharmacy) at Universiti Teknologi MARA, Malaysia. The authors acknowledge the Government of Malaysia for providing financial support through the Ministry of Higher Education under grants no. RMI 600-RMI/ERGS 5/3 (36/2013) and 600-RMI/FRGS 5/3 (111/2014).

The authors declare that there are no competing interests. All authors have jointly designated associate professor Dr. Igor Iezhitsa to be responsible for decisions regarding the presence and the order of the authors in the manuscript. Dr. Igor Iezhitsa has also been selected by all authors to be responsible for all future communication with the journal regarding this manuscript.

REFERENCES

Albers GW, Bogousslavsky J, Bozik MA, Brass LM, Broderick JP, Fisher M, Goldstein LB, Salazar-Grueso E, Zivin JA (2001) Recommendations for clinical trial evaluation of acute stroke therapies. Stroke 32: 1598–1606.

Aziz ZA, Lee YY, Ngah BA, Sidek NN, Looi I, Hanip MR, Basri HB (2015) Acute stroke registry Malaysia, 2010–2014: results from the National Neurology Registry. J Stroke Cerebrovasc Dis 24: 2701–2709.

Baron JC, Yamauchi H, Fujioka M, Endres M (2014) Selective neuronal loss in ischemic stroke and cerebrovascular disease. J Cereb Blood Flow Metab 34: 2–18.

Barone FC, Feuerstein GZ (1999) Inflammatory mediators and stroke: new opportunities for novel therapeutics. J Cereb Blood Flow Metab 19: 819–834.

Baydyuk M, Xu B (2014) BDNF signaling and survival of striatal neurons. Front Cell Neurosci 8: 254.

Belayev L, Busto R, Zhao W, Fernandez G, Ginsberg MD (1999) Middle cerebral artery occlusion in the mouse by intraluminal suture coated with poly-L-lysine: neurological and histological validation. Brain Res 833: 181–190.

Betz AL, Firth JA, Goldstein GW (1980) Polarity of the blood-brain barrier: distribution of enzymes between the luminal and antiluminal membranes of brain capillary endothelial cells. Brain Res 192: 17–28.

Betz AL, Goldstein GW (1978) Polarity of the blood-brain barrier: neutral amino acid transport into isolated brain capillaries. Science 202: 225–227.

Bharosay A, Bharosay VV, Saxena K, Varma M (2018) Role of brain biomarker in predicting clinical outcome in hypertensive cerebrovascular ischemic stroke. Indian J Clin Biochem 2017: 1–6.

Boltze J, Schmidt UR, Reich DM, Kranz A, Reymann KG, Strassburger M, Lobsien D, Wagner DC, Förschler A, Schäbitz WR (2012) Determination of the therapeutic time window for human umbilical cord blood mononuclear cell transplantation following experimental stroke in rats. Cell Transplant 21: 1199–1211.

Çakmak VA, Gündüz A, Karaca Y, Alioğlu Z, Menteşe A, Topbaş M (2014) Diagnostic significance of ischemia-modified albumin, S100b, and neuron-specific enolase in acute ischemic stroke. Akademik Acil Tip Olgu Sunumlari Dergisi 13: 112–117.

Carmichael ST (2005) Rodent models of focal stroke: size, mechanism, and purpose. NeuroRx 2: 396–409.

Casmiro M, Maitan S, De Pasquale F, Cova V, Scarpa E, Vignatelli L, NSE Study Group (2005) Cerebrospinal fluid and serum neuron-specific enolase concentrations in a normal population. Eur J Neuro 12: 369–374.

Çeltik C, Acunaş B, Öner N, Pala Ö (2004) Neuron-specific enolase as a marker of the severity and outcome of hypoxic ischemic encephalopathy. Brain Dev 26: 398–402.

Chabok SY, Moghadam AD, Saneei Z, Amlashi FG, Leili EK, Amiri ZM (2012) Neuron-specific enolase and S100BB as outcome predictors in severe diffuse axonal injury. J Trauma Acute Care Surg 72: 1654–1657.

Chan DK, Levi C, Cordato D, O'Rourke F, Chen J, Redmond H, Xu YH, Middleton S, Pollack M, Hankey GJ (2014) Health service management study for stroke: a randomized controlled trial to evaluate two models of stroke care. Int J Stroke 9: 400–405.

Chao MV (2003) Neurotrophins and their receptors: a convergence point for many signalling pathways. Nat Rev Neurosci 4: 299–309.

Chao OY, Pum ME, Li JS, Huston JP (2012) The grid-walking test: assessment of sensorimotor deficits after moderate or severe dopamine depletion by 6-hydroxydopamine lesions in the dorsal striatum and medial forebrain bundle. Neuroscience 202: 318–325.

Chen A, Lin Z, Lan L, Xie G, Huang J, Lin J, Peng J, Tao J, Chen L (2012) Electroacupuncture at the Quchi and Zusanli acupoints exerts neuroprotective role in cerebral ischemia-reperfusion injured rats *via* activation of the PI3K/Akt pathway. Int J Mol Med 30: 791–796.

Chen A, Xiong LJ, Tong Y, Mao M (2013a) Neuroprotective effect of brain-derived neurotrophic factor mediated by autophagy through the PI3K/Akt/mTOR pathway. Mol Med Rep 8: 1011–1016.

Chen AI, Xiong LJ, Tong YU, Mao M (2013b) The neuroprotective roles of BDNF in hypoxic ischemic brain injury. Biomed Rep 1: 167–176.

Chen J, Sanberg PR, Li Y, Wang L, Lu M, Willing AE, Sanchez-Ramos J, Chopp M (2001) Intravenous administration of human umbilical cord blood reduces behavioral deficits after stroke in rats. Stroke 32: 2682–2688.

Chen J, Zacharek A, Zhang C, Jiang H, Li Y, Roberts C, Lu M, Kapke A, Chopp M (2005) Endothelial nitric oxide synthase regulates brain-derived neurotrophic factor expression and neurogenesis after stroke in mice. J Neurosci 25: 2366–2375.

Chen J, Zhang C, Jiang H, Li Y, Zhang L, Robin A, Katakowski M, Lu M, Chopp M (2005) Atorvastatin induction of VEGF and BDNF promotes brain plasticity after stroke in mice. J Cereb Blood Flow Metab 25: 281–290.

Chiamulera C, Terron A, Reggiani A, Cristofori P (1993) Qualitative and quantitative analysis of the progressive cerebral damage after middle cerebral artery occlusion in mice. Brain Res 606: 251–258.

Cunningham RT, Young IS, Winder J, O'Kane MJ, McKinstry S, Johnston CF, Dolan OM, Hawkins SA, Buchanan KD (1991) Serum neurone specific enolase (NSE) levels as an indicator of neuronal damage in patients with cerebral infarction. Eur J Clin Invest 21: 497–500.

Ejaz S, Williamson DJ, Ahmed T, Sitnikov S, Hong YT, Sawiak SJ, Fryer TD, Aigbirhio FI, Baron JC (2013) Characterizing infarction and selective neuronal loss following temporary focal cerebral ischemia in the rat: a multi-modality imaging study. Neurobiol Dis 51: 120–132.

Elting JW, de Jager AE, Teelken AW, Schaaf MJ, Maurits NM, van der Naalt J, Sibinga CT, Sulter GA, De Keyser J (2000) Comparison of serum S-100 protein levels following stroke and traumatic brain injury. J Neurol Sci 181: 104–110.

Freret T, Bouet V, Leconte C, Roussel S, Chazalviel L, Divoux D, Schumann-Bard P, Boulouard M (2009) Behavioral deficits after distal focal cerebral ischemia in mice: Usefulness of adhesive removal test. Behav Neurosci 123: 224–230.

Fulle S, Pietrangelo T, Mariggio MA, Lorenzon P, Racanicchi L, Mozrzymas J, Guarnieri S, Zucconi-Grassi G, Fano G (2000) Calcium and fos involvement in brain-derived Ca2+-binding protein (S100)-dependent apoptosis in rat phaeochromocytoma cells. Exp Physiol 85: 243–253.

Ga D, Fisher M, Macleod M, Davis SM (2008) Stroke. Lancet 371: 1612–1623.

Garcia JH, Lassen NA, Weiller C, Sperling B, Nakagawara J (1996) Ischemic stroke and incomplete infarction. Stroke 27: 761–765.

Garcia JH, Liu KF, Ye ZR, Gutierrez JA (1997) Incomplete infarct and delayed neuronal death after transient middle cerebral artery occlusion in rats. Stroke 28: 2303–2310.

Garcia JH, Wagner S, Liu KF, Hu XJ (1995) Neurological deficit and extent of neuronal necrosis attributable to middle cerebral artery occlusion in rats: statistical validation. Stroke 26: 627–635.

Gelderblom M, Daehn T, Schattling B, Ludewig P, Bernreuther C, Arunachalam P, Matschke J, Glatzel M, Gerloff C, Friese MA, Magnus T (2013) Plasma levels of neuron specific enolase quantify the extent of neuronal injury in murine models of ischemic stroke and multiple sclerosis. Neurobiol Dis 59: 177–182.

Gelperina S, Maksimenko O, Khalansky A, Vanchugova L, Shipulo E, Abbasova K, Berdiev R, Wohlfart S, Chepurnova N, Kreuter J (2010) Drug delivery to the brain using surfactant-coated poly (lactide-co-glycolide) nanoparticles: influence of the formulation parameters. Eur J Pharm Biopharm 74: 157–163.

Goldlust EJ, Paczynski RP, He YY, Hsu CY, Goldberg MP (1996) Automated measurement of infarct size with scanned images of triphenyltetrazolium chloride-stained rat brains. Stroke 27: 1657–1662.

Goldstein GW, Betz AL (1986) The blood-brain barrier. Sci Am 255: 74–83.

Guo C, Zhu Y, Weng Y, Wang S, Guan Y, Wei G, Yin Y, Xi M, Wen A (2014) Therapeutic time window and underlying therapeutic mechanism of breviscapine injection against cerebral ischemia/reperfusion injury in rats. J Ethnopharmacol 151: 660–666.

Guo ZV, Li N, Huber D, Ophir E, Gutnisky D, Ting JT, Feng G, Svoboda K (2014) Flow of cortical activity underlying a tactile decision in mice. Neuron 81: 179–194.

Gupta S, Sharma U, Jagannathan NR, Gupta YK (2017) Neuroprotective effect of lercanidipine in middle cerebral artery occlusion model of stroke in rats. Exp Neurol 288: 25–37.

Haley MJ, Lawrence CB (2017) The blood–brain barrier after stroke: structural studies and the role of transcytotic vesicles. J Cereb Blood Flow Metab 37: 456–470.

Han BH, D'Costa A, Back SA, Parsadanian M, Patel S, Shah AR, Gidday JM, Srinivasan A, Deshmukh M, Holtzman DM (2000) BDNF blocks caspase-3 activation in neonatal hypoxia-ischemia. Neurobiol Dis 7: 38–53.

Han JC, Thurm A, Williams CG, Joseph LA, Zein WM, Brooks BP, Butman JA, Brady SM, Fuhr SR, Hicks MD, Huey AE (2013) Association of brain-derived neurotrophic factor (BDNF) haploinsufficiency with lower adaptive behaviour and reduced cognitive functioning in WAGR/11p13 deletion syndrome. Cortex 49: 2700–2710.

Hårdemark HG, Ericsson N, Kotwica Z, Rundström G, Mendel-Hartvig I, Olsson Y, Påhlman S, Persson L (1989) S-100 protein and neuron-specific enolase in CSF after experimental traumatic or focal ischemic brain damage. J Neurosurgery 71*:* 727–731.

Hatfield RH, Mendelow AD, Perry RH, Alvarezs LM, Modha P (1991) Triphenyltetrazolium chloride (TTC) as a marker for ischaemic changes in rat brain following permanent middle cerebral artery occlusion Neuropathol Appl Neurobiol 17: 61–67.

Hernandez TD, Schallert T (1988) Seizures and recovery from experimental brain damage. Exp Neurol 102: 318–324.

Horn M, Seger F, Schlote W (1995) Neuron-specific enolase in gerbil brain and serum after transient cerebral ischemia. Stroke 26: 290–297.

Hu J, Ferreira A, Van Eldik LJ (1997) S100β induces neuronal cell death through nitric oxide release from astrocytes J Neurochem 69: 2294–2301.

Jauch EC, Barreto AD, Broderick JP, Char DM, Cucchiara BL, Devlin TG, Haddock AJ, Hicks WJ, Hiestand BC, Jickling GC, June J (2017) Biomarkers of acute stroke etiology (BASE) study methodology. Transl Stroke Res 8: 424–428.

Jiang Y, Wei N, Zhu J, Lu T, Chen Z, Xu G, Liu X (2010) Effects of brain-derived neurotrophic factor on local inflammation in experimental stroke of rat. Mediators Inflamm 2010: 372423.

Joshi CN, Jain SK, Murthy PS (2004) An optimized triphenyltetrazolium chloride method for identification of cerebral infarcts. Brain Res Brain Res Protoc 13: 11–17.

Kanemitsu H, Nakagomi T, Tamura A, Tsuchiya T, Kono G, Sano K (2002) Differences in the extent of primary ischemic damage between middle cerebral artery coagulation and intraluminal occlusion models. J Cereb Blood Flow Metab 22: 1196–1204.

Kim JY, Ho H, Kim N, Liu J, Tu CL, Yenari MA, Chang W (2014) Calcium-sensing receptor (CaSR) as a novel target for ischemic neuroprotection. Ann Clin Transl Neurol 1: 851–866.

Koizumi JY, Yoshida Y, Nakazawa T, Ooneda G (1986) Experimental studies of ischemic brain edema. Jpn J Stroke 8: 1–8.

Koppal T, Lam AG, Guo L, Van Eldik LJ (2001) S100B proteins that lack one or both cysteine residues can induce inflammatory responses in astrocytes and microglia. Neurochem Int 39: 401–407.

Krueger M, Härtig W, Reichenbach A, Bechmann I, Michalski D (2013) Blood-brain barrier breakdown after embolic stroke in rats occurs without ultrastructural evidence for disrupting tight junctions. PLoS One 8: e56419.

Kulkarni SA, Feng SS (2011) Effects of surface modification on delivery efficiency of biodegradable nanoparticles across the blood–brain barrier. Nanomedicine 6: 377–394.

Kume T, Kouchiyama H, Kaneko S, Maeda T, Kaneko S, Akaike A, Shimohama S, Kihara T, Kimura J, Wada K, Koizumi S (1997) BDNF prevents NO mediated glutamate cytotoxicity in cultured cortical neurons. Brain Res 756: 200–204.

Lee S, Lee M, Hong Y, Won J, Lee Y, Kang SG, Chang KT, Hong Y (2014) Middle cerebral artery occlusion methods in rat *versus* mouse models of transient focal cerebral ischemic stroke. Neural Regen Res 9: 757.

Lee S, Shin J, Lee M, Hong Y, Lee SK, Lee Y, Lkhagvasuren T, Kim DW, Yang YA, Chang KT, Hong Y (2012) Melatonin combined with exercise cannot alleviate cerebral injury in a rat model of focal cerebral ischemia/reperfusion injury. Neural Regen Res 7: 993–999.

Li K, Jia J, Wang Z, Zhang S (2015) Elevated serum levels of NSE and S-100β correlate with increased risk of acute cerebral infarction in Asian populations. Med Sci Monit 21: 1879–1888.

Li Y, Chopp M, Jiang N, Yao F, Zaloga C (1995) Temporal profile of in situ DNA fragmentation after transient middle cerebral artery occlusion in the rat. J Cereb Blood Flow Metab 15: 389–397.

Li YI, Chen J, Zhang CL, Wang L, Lu D, Katakowski M, Gao Q, Shen LH, Zhang J, Lu M, Chopp M (2005) Gliosis and brain remodeling after treatment of stroke in rats with marrow stromal cells. Glia 49: 407–417.

Liu F, Schafer DP, McCullough LD (2009) TTC, fluoro-Jade B and NeuN staining confirm evolving phases of infarction induced by middle cerebral artery occlusion. J Neurosci Methods 179: 1–8.

Liu S, Zhen G, Meloni BP, Campbell K, Winn HR (2009) Rodent stroke model guidelines for preclinical stroke trials. J Exp Stroke Transl Med 2: 2–27.

Lo EH, Dalkara T, Moskowitz MA (2003) Neurological diseases: Mechanisms, challenges and opportunities in stroke. Nat Rev Neurosci 4: 399–415.

Lu B, Nagappan G, Guan X, Nathan PJ, Wren P (2013) BDNF-based synaptic repair as a disease-modifying strategy for neurodegenerative diseases. Nat Rev Neurosci 14: 401–416.

Lu B, Nagappan G, Lu Y (2014) BDNF and synaptic plasticity, cognitive function, and dysfunction. Handb Exp Pharmacol 220: 223–250.

Mabe H, Suzuki S, Mase M, Umemura A, Nagai H (1991) Serum neuron-specific enolase levels after subarachnoid hemorrhage. Surg Neurol 36: 170–174.

Martens P, Raabe A, Johnsson P (1998). Serum S-100 and neuron-specific enolase for prediction of regaining consciousness after global cerebral ischemia. Stroke 29: 2363–2366.

Matsui T, Mori T, Tateishi N, Kagamiishi Y, Satoh S, Katsube N, Morikawa E, Morimoto T, Ikuta F, Asano T (2002) Astrocytic activation and delayed infarct expansion after permanent focal ischemia in rats. Part I: enhanced astrocytic synthesis of S-100β in the periinfarct area precedes delayed infarct expansion. J Cereb Blood Flow Metab 22: 711–722.

Meng L, Liu B, Ji R, Jiang X, Yan X, Xin Y (2019) Targeting the BDNF/TrkB pathway for the treatment of tumors Oncol Lett 17: 2031–2039.

Mergenthaler P, Meisel A (2012) Do stroke models model stroke? Dis Model Mech 5: 718–725.

Missler U, Wiesmann M, Friedrich C, Kaps M (1997) S-100 protein and neuron-specific enolase concentrations in blood as indicators of infarction volume and prognosis in acute ischemic stroke. Stroke 28: 1956–1960.

Moghimi SM, Hunter AC (2000) Poloxamers and poloxamines in nanoparticle engineering and experimental medicine. Trends Biotechnol 18: 412–420.

Mori T, Koyama N, Arendash GW, Horikoshi-Sakuraba Y, Tan J, Town T (2010) Overexpression of human S100B exacerbates cerebral amyloidosis and gliosis in the Tg2576 mouse model of Alzheimer's disease. Glia 58: 300–314.

Mozafari MR, Pardakhty A, Azarmi S, Jazayeri JA, Nokhodchi A, Omri A (2009) Role of nanocarrier systems in cancer nanotherapy. J Liposome Res 19: 310–321.

Murer MG, Yan Q, Raisman-Vozari R (2001) Brain-derived neurotrophic factor in the control human brain, and in Alzheimer's disease and Parkinson's disease. Prog Neurobiol 63: 71–124.

Nagahara AH, Tuszynski MH (2011) Potential therapeutic uses of BDNF in neurological and psychiatric disorders. Nat Rev Drug Discov 10: 209–219.

Nahirney PC, Reeson P, Brown CE (2016) Ultrastructural analysis of blood-brain barrier breakdown in the peri-infarct zone in young adult and aged mice. J Cereb Blood Flow Metab 36: 413–425.

Nash DL, Bellolio MF, Stead LG (2008) S100 as a marker of acute brain ischemia: a systematic review. Neurocrit Care 8: 301–307.

Ohira K, Hayashi M (2009) A new aspect of the TrkB signaling pathway in neural plasticity. Curr Neuropharmacol 7: 276–285.

Olivecrona Z, Bobinski L, Koskinen LO (2015) Association of ICP, CPP, CT findings and S-100B and NSE in severe traumatic head injury. Prognostic value of the biomarkers. Brain Inj 29: 446–454.

Oron A, Oron U, Chen J, Eilam A, Zhang C, Sadeh M, Lampl Y, Streeter J, DeTaboada L, Chopp M (2006) Low-level laser therapy applied transcranially to rats after induction of stroke significantly reduces long-term neurological deficits. Stroke 37: 2620–2624.

Park HS, Han KH, Shin JA, Park JH, Song KY, Kim DH (2014) The neuroprotective effects of carnosine in early stage of focal ischemia rodent model. J Korean Neurosurg Soc 55: 125–130.

Park JS, Shin JA, Jung JS, Hyun JW, Van Le TK, Kim DH, Park EM, Kim HS (2012) Anti-inflammatory mechanism of compound K in activated mi-

croglia and its neuroprotective effect on experimental stroke in mice. J Pharmacol Exp Ther 341: 59–67.

Patel RA, McMullen PW (2017) Neuroprotection in the treatment of acute ischemic stroke. Prog Cardiovasc Dis 59: 542–548.

Persson L, Hårdemark HG, Gustafsson J, Rundström G, Mendel-Hartvig IB, Esscher T, Påhlman S (1987) S-100 protein and neuron-specific enolase in cerebrospinal fluid and serum: markers of cell damage in human central nervous system. Stroke 18: 911–918.

Poduslo JF, Curran GL (1996) Permeability at the blood-brain and blood-nerve barriers of the neurotrophic factors: NGF, CNTF, NT-3, BDNF. Brain Res Mol Brain 36: 280–286.

Popp A, Jaenisch N, Witte OW, Frahm C (2009) Identification of ischemic regions in a rat model of stroke. PloS One 4: e4764.

Rogers DC, Campbell CA, Stretton JL, Mackay KB (1997a) Correlation between motor impairment and infarct volume after permanent and transient middle cerebral artery occlusion in the rat. Stroke 28: 2060–2066.

Rogers DC, Fisher EM, Brown SD, Peters J, Hunter AJ, Martin JE (1997b) Behavioral and functional analysis of mouse phenotype: SHIRPA, a proposed protocol for comprehensive phenotype assessment. Mamm Genome 8: 711–713.

Sahu S, Nag DS, Swain A, Samaddar DP (2017) Biochemical changes in the injured brain. World J Biol Chem 8: 21.

Sandoval KE, Witt KA (2008) Blood-brain barrier tight junction permeability and ischemic stroke. Neurobiol Dis 32: 200–219.

Saraiva C, Praça C, Ferreira R, Santos T, Ferreira L, Bernardino L (2016) Nanoparticle-mediated brain drug delivery: overcoming blood-brain barrier to treat neurodegenerative diseases. J Control Release 235: 34–47.

Schaar KL, Brenneman MM, Savitz SI (2010) Functional assessments in the rodent stroke model. Exp Transl Stroke Med 2: 13.

Schabitz WR, Berger C, Kollmar R, Seitz M, Tanay E, Kiessling M, Schwab S, Sommer C (2004) Effect of brain-derived neurotrophic factor treatment and forced arm use on functional motor recovery after small cortical ischemia. Stroke 35: 992–997.

Schäbitz WR, Schwab S, Spranger M, Hacke W (1997) Intraventricular brain-derived neurotrophic factor reduces infarct size after focal cerebral ischemia in rats. J Cereb Blood Flow Metab 17: 500–506.

Schabitz WR, Sommer C, Zoder W, Kiessling M, Schwaninger M, Schwab S (2000) Intravenous brain-derived neurotrophic factor reduces infarct size and counterregulates Bax and Bcl-2 expression after temporary focal cerebral ischemia. Stroke 31: 2212–2216.

Schwengel K, Namsolleck P, Lucht K, Clausen BH, Lambertsen KL, Valero-Esquitino V, Thöne-Reineke C, Müller S, Widdop RE, Denton KM, Horiuchi M (2016) Angiotensin AT2-receptor stimulation improves survival and neurological outcome after experimental stroke in mice. J Mol Med 94: 957–966.

Shukla PK, Khanna VK, Ali MM, Maurya R, Khan MY, Srimal RC (2006) Neuroprotective effect of Acorus calamus against middle cerebral artery occlusion–induced ischaemia in rat. Hum Exp Toxicol 25: 187–194.

Skogseid IM, Nordby HK, Urdal P, Paus E, Lilleaas F (1992) Increased serum creatine kinase BB and neuron specific enolase following head injury indicates brain damage. Acta Neurochir 115: 106–111.

Sorci G, Riuzzi F, Arcuri C, Tubaro C, Bianchi R, Giambanco I, Donato R (2013) S100B protein in tissue development, repair and regeneration. World J Biol Chem 4: 1–12.

Steiner J, Bogerts B, Schroeter ML, Bernstein HG (2011) S100B protein in neurodegenerative disorders. Clin Chem Lab Med 49: 409–424.

Stokum JA, Gerzanich V, Simard JM (2016) Molecular pathophysiology of cerebral edema. J Cereb Blood Flow Metab 36: 513–538.

Sun J, Wang F, Li H, Zhang H, Jin J, Chen W, Pang M, Yu J, He Y, Liu J, Liu C (2015) Neuroprotective effect of sodium butyrate against cerebral ischemia/reperfusion injury in mice. Biomed Res Int 2015: 395895.

Swanson RA, Morton MT, Tsao-Wu G, Savalos RA, Davidson C, Sharp FR (1990) A semiautomated method for measuring brain infarct volume. J Cereb Blood Flow Metab 10: 290–293.

Taliyan R, Ramagiri S (2016) Delayed neuroprotection against cerebral ischemia reperfusion injury: putative role of BDNF and GSK-3β. J Recept Signal Transduct Res 36: 402–410.

Tanaka Y, Koizumi C, Marumo T, Omura T, Yoshida S (2007) Serum S100B is a useful surrogate marker for long-term outcomes in photochemically-induced thrombotic stroke rat models. Life Sci 81: 657–663.

Tanaka Y, Marumo T, Omura T, Yoshida S (2007) Early increases in serum S100B are associated with cerebral hemorrhage in a rat model of focal cerebral ischemia. Brain Res 1227: 248–254.

Tawk RG, Grewal SS, Heckman MG, Rawal B, Miller DA, Edmonston D, Ferguson JL, Navarro R, Ng L, Brown BL, Meschia JF (2015) The relationship between serum neuron-specific enolase levels and severity of bleeding and functional outcomes in patients with nontraumatic subarachnoid hemorrhage. Neurosurgery 78: 487–491.

Thoenen H (1995) Neurotrophins and neuronal plasticity. Science 270: 593–598.

Thorne RG, Frey WH (2001) Delivery of neurotrophic factors to the central nervous system. Clin Pharmacokinet 40: 907–946.

Traudt CM, Juul SE (2013) Erythropoietin as a neuroprotectant for neonatal brain injury: animal models. Methods Mol Biol 982: 113–126.

Tsivgoulis G, Katsanos AH, Alexandrov AV (2014) Reperfusion therapies of acute ischemic stroke: potentials and failures. Front Neurol 5: 215.

Villa RF, Gorini A, Hoyer S (2009). Effect of ageing and ischemia on enzymatic activities linked to Krebs' cycle, electron transfer chain, glutamate and aminoacids metabolism of free and intrasynaptic mitochondria of cerebral cortex. Neurochem Res 34: 2102.

Wang CC, Chio CC, Chang CH, Kuo JR, Chang CP (2010) Beneficial effect of agmatine on brain apoptosis, astrogliosis, and edema after rat transient cerebral ischemia. BMC Pharmacol 10: 11.

Williams AJ, Berti R, Dave JR, Elliot PJ, Adams J, Tortella FC (2004) Delayed treatment of ischemia/reperfusion brain injury: extended therapeutic window with the proteosome inhibitor MLN519. Stroke 35: 1186–1191.

Wohlfart S, Khalansky AS, Gelperina S, Maksimenko O, Bernreuther C, Glatzel M, Kreuter J (2011) Efficient chemotherapy of rat glioblastoma using doxorubicin-loaded PLGA nanoparticles with different stabilizers. PloS One 6: e19121.

World Health Organization (2002) World Health Reports "Reducing risks, promoting healthy life". Geneva.

Yamashita K, Wiessner C, Lindholm D, Thoenen H, Hossmann KA (1997) Post-occlusion treatment with BDNF reduces infarct size in a model of permanent occlusion of the middle cerebral artery in rat. Metab Brain Dis 12: 271–280.

Yang Y, Rosenberg GA (2011) MMP-mediated disruption of claudin-5 in the blood–brain barrier of rat brain after cerebral ischemia. Methods Mol Biol 762: 333–345.

Yi YH, Guo WC, Sun WW, Su T, Lin H, Chen SQ, Deng WY, Zhou W, Liao WP (2008) Neuroprotection of lamotrigine on hypoxic-ischemic brain damage in neonatal rats: Relations to administration time and doses. Biologics 2: 339–344.

Yrjänheikki J, Tikka T, Keinänen R, Goldsteins G, Chan PH, Koistinaho J (1999) A tetracycline derivative, minocycline, reduces inflammation and protects against focal cerebral ischemia with a wide therapeutic window. Proc Natl Acad Sci 96: 13496–13500.

Zaheer S, Beg M, Rizvi I, Islam N, Ullah E, Akhtar N (2013) Correlation between serum neuron specific enolase and functional neurological outcome in patients of acute ischemic stroke. Ann Indian Acad Neurol 16: 504–508.

Zensi A, Begley D, Pontikis C, Legros C, Mihoreanu L, Wagner S, Büchel C, Kreuter J (2009) Albumin nanoparticles targeted with Apo E enter the CNS by transcytosis and are delivered to neurones. J Control Release 137: 78–86.

Zhang L, Zhang RL, Jiang Q, Ding G, Chopp M, Zhang ZG (2015) Focal embolic cerebral ischemia in the rat. Nat Protoc 10: 539–547.

Zhang R, Zhang Z, Zhang C, Zhang L, Robin A, Wang Y, Lu M, Chopp M (2004) Stroke transiently increases subventricular zone cell division from asymmetric to symmetric and increases neuronal differentiation in the adult rat. J Neurosci 24: 5810–5815.

Zhang X, Zhou Y, Li H, Wang R, Yang D, Li B, Fu J (2018a) Intravenous administration of DPSCs and BDNF improves neurological performance in rats with focal cerebral ischemia. Int J Mol Med 41: 3185–3194.

Zhang JH, Li JK, Ma LL, Lou JY (2018b) RNA interference-mediated silencing of S100B improves nerve function recovery and inhibits hippocampal cell apoptosis in rat models of ischemic stroke. J Cell Biochem 119: 8095–8111.

Zhang Y, Pardridge WM (2001) Conjugation of brain-derived neurotrophic factor to a blood-brain barrier drug targeting system enables neuroprotection in regional brain ischemia following intravenous injection of the neurotrophin. Brain Res 889: 49–56.

Zhang Y, Pardridge WM (2006) Blood–brain barrier targeting of BDNF improves motor function in rats with middle cerebral artery occlusion. Brain Res 1111: 227–229.